

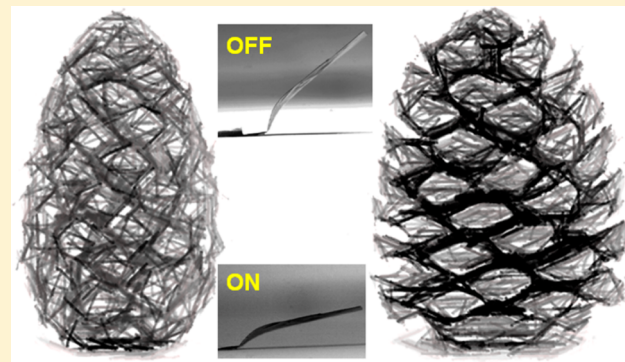
Shape-Morphing Nanocomposite Origami

Christine M. Andres, Jian Zhu, Terry Shyu, Connor Flynn, and Nicholas A. Kotov*

Department of Chemical Engineering, University of Michigan, Ann Arbor, Michigan 48109, United States

Supporting Information

ABSTRACT: Nature provides a vast array of solid materials that repeatedly and reversibly transform in shape in response to environmental variations. This property is essential, for example, for new energy-saving technologies, efficient collection of solar radiation, and thermal management. Here we report a similar shape-morphing mechanism using differential swelling of hydrophilic polyelectrolyte multilayer inkjets deposited on an LBL carbon nanotube (CNT) composite. The out-of-plane deflection can be precisely controlled, as predicted by theoretical analysis. We also demonstrate a controlled and stimuli-responsive twisting motion on a spiral-shaped LBL nanocomposite. By mimicking the motions achieved in nature, this method offers new opportunities for the design and fabrication of functional stimuli-responsive shape-morphing nanoscale and microscale structures for a variety of applications.



INTRODUCTION

Stimuli-responsive materials able to convert external stimuli reversibly to three-dimensional (3D) mechanical motion have attracted significant attention for their potential to enable controllable and programmable shape morphing.^{1,2} Great success has been achieved in utilizing stimuli-responsive materials for the self-assembly of 3D structures³ and the realization of shape-memory polymers.⁴ However, in many cases the self-assembled 3D structures are not designed to disassemble, and shape-memory polymers require a reprogramming cycle for repeated response.^{3,4} Dynamically tunable materials capable of repeatedly and reversibly converting simple environmental stimuli into mechanical motion are of interest for developments in adaptable clothing,⁵ climate-responsive buildings,⁶ controlled encapsulation/delivery,⁷ solar tracking in photovoltaic farms, and the actuation of soft robotics.⁸

Most living systems are capable of repeatedly responding to changes in their environment with a series of mechanical reconfigurations. The ability to fabricate synthetic materials that meet or exceed these capabilities is a substantial and significant engineering challenge.^{9–11} Although some biological movements require complicated chemical and biological mechanisms, several plants demonstrate mechanoresponsive behaviors for seed dispersal that are deceptively simple and independent of cellular mechanisms.^{12–16} For example, an investigation into the mechanisms of unfolding/folding of pine cones^{12,17} and ice plants¹³ has revealed that they are based on a simple mechanism of differential swelling in response to variations in relative humidity. The simple change in humidity is able to create a complex mechanical response due to the controlled composition and structural attributes of the plant material. Here a cellulosic inner layer organized in a stratified structure is capable of absorbing large amounts of water. Paired with an opposing tissue that has a different cellulose fibril orientation that restricts the

swelling behavior, a bending moment is generated.¹³ Similar to the uniform heating of bimetallic strips,¹⁸ the difference in expansion coefficients does not allow for uniform expansion, and the internal stresses are equilibrated with a bending moment. The location of the bimorph within the plant creates a hinged structure where origami-like folding is realized. Upon removal of the stimulus, the bimorph will return to its original shape, providing a straightforward way to create reversible and repeatable shape-morphing structures.

Reversible shape transformations from the differential swelling of synthetic bimorph structures in solution have been widely observed.^{19–23} Differential swelling in hydrogel-based materials is a prominent example. In solution, their elastic networks allow for significant volume change based on polymer hydration and chain mobility.^{24–26} However, such a response to humidity outside of solution²⁷ is difficult for solid synthetic networks where the increased stiffness imposes larger restrictions on chain mobility within the network, directly limiting responsiveness.²⁸

The nanoscale structural control and versatility of layer-by-layer (LBL) assembly²⁹ has been proven to be a simple technique for the fabrication of solid functional materials that respond to a variety of external stimuli.³⁰ In most cases, these materials have been applied to trigger morphological changes on flat surfaces or to control the permeability of capsules within solution. Surprisingly, little investigation into freestanding structures that can generate mechanical motion outside of solution has been performed.^{31–33} In addition to the fabrication of stimuli-responsive materials, LBL has also been employed to fabricate a wide variety of nanocomposites with very distinctive mechanical,

Received: January 4, 2014

Revised: February 25, 2014

Published: April 1, 2014

electrical, biological, thermal, and optical properties.^{34–39} Although traditionally a technique used to fabricate planar thin films, the introduction of multiscale and multidimensional patterning to create permanent shapes^{38,40–42} has been developed as an important step toward the incorporation of such materials into advanced functional devices. The next logical step is the incorporation of advanced stimuli-responsive functionality into such nanocomposite structures.

Herein we present LBL-assembled solid polymeric multilayers capable of driving shape transformations in response to environmental humidity and temperature variations. A hydrophilic polyelectrolyte multilayer is stacked with a less-responsive LBL-assembled carbon nanotube (CNT) composite. The differential swelling of the two LBL layers results in repeatable and reversible out-of-plane deformations. The sorption properties of polyelectrolyte multilayers are then revealed to drive a pseudonegative thermal expansion⁴³ that is applied to drive similar shape morphing with temperature variations. In agreement with a theoretical model, the ability of LBL assembly to control thickness on the nanoscale allows for the responsive behavior of the material to be strictly controlled. LBL deposition by inkjet⁴⁰ is employed to pattern the active material onto the base in order to localize the stresses for programmable folding. Finally, a biomimetic structure is fabricated for the realization of a 3D responsive structure as inspired by the awn of wheat grass or tendrils of climbing plants.

■ EXPERIMENTAL SECTION

Fabrication of LBL Nanocomposite. In a typical LBL cycle, glass slides cleaned by piranha solution for 24 h were immersed in 1% cationic polyurethane (Hepce Chem Co., South Korea, $M_w \sim 92\,000$) for 5 min, rinsed with deionized water, and then dried with compressed air. Subsequently, these slides were dipped into 0.25 mg/mL P3 single-walled carbon nanotube (SWNT, Carbon Solution Inc.) aqueous dispersions for 5 min, followed by rinsing and drying. The P3 SWNTs were well dispersed in water by sonicating for 20 min. Two hundred bilayer films were deposited on a glass substrate by a NanoStrata robot. The (PU/CNT)₂₀₀ films were then removed with brief exposure to hydrofluoric acid.

Analysis of Thermal Expansion Properties. High-molecular-weight poly(diallyldimethylammonium) chloride (PDDA) and poly(sodium 4-styrenesulfonate) (PSS, $M_w 70\,000$) were purchased from Aldrich and diluted with deionized water. A (PDDA/PSS)₂₅₀ film was fabricated on a Teflon substrate with 1 wt % solutions of each polyelectrolyte using the typical LBL cycle described above. Upon removal from Teflon, the films were stacked 4-fold before hot pressing under four tons at 80 °C for 5 h to obtain a film thick enough to withstand characterization. The hot-pressed (PDDA/PSS) film and the (PU/CNT)₂₀₀ film were cut into 2-mm-wide and 15-mm-long strips for thermal mechanical analysis.

The coefficient of thermal expansion, α , of the film was measured in extension mode with a PerkinElmer TMA7 following the ASTM test method for the linear thermal expansion of solid materials by thermomechanical analysis (E 831) and slightly modified to measure thin films.^{44,45} The extension probe and grips were customized by RT Instruments, Inc. to minimize the expansion of the grips during the measurement. Ultrapure helium was used as a purge gas to give an inert atmosphere and facilitate heat transfer. Cooling of the chamber was accomplished by circulating water at 8 °C provided by a chiller. The TMA instrument was calibrated using an aluminum standard; the experimental error for α of aluminum was 7.6% for temperatures as high as 300 °C. The α of Kevlar fibers from DuPont was also measured as an additional calibration for negative expansion, yielding a value of -4.58 ppm/°C, which is in agreement with data reported elsewhere.⁴⁶

The strips were stretched under 45 mN of force, and the length changes were recorded by monitoring the probe displacement for temperature ramps of 5 °C/min. The sample was initially heated from 30 to 80 °C and then stabilized for 2 h to remove free water and residual

stress. The length change for both cooling and heating segments was used to calculate α , represented by the slope of the curve normalized by the initial length at 30 °C. Average α values were calculated from the 75–35 °C interval. More than three samples were measured for each data point. For varied humidity testing, relative humidity values of approximately 7.7, 2.5, 1.4, 0.7, and 0.4% were achieved with a controlled flow of ultrapure 99.9995% helium.

Inkjet Deposition of Polyelectrolyte Multilayers. PDDA and PSS were diluted in deionized water to 0.025 wt % and sent through 0.22 μm filters. Two 10 pL droplet size cartridges with 16 piezoelectric nozzles were loaded separately with each polyelectrolyte. A FUJIFILM Dimatix material printer (DMP-2800) was used to deliver both polyelectrolytes to the surface with a typical voltage cycle (waveform) with two steps at a duration of 5.056 μs each. First, a slew rate of 0.9 was applied to reach a level of 87%, followed by a slew rate of 0.19 decreasing to 0%. The waveform was fired at a frequency of 5 kHz. Cartridge settings were set to a print height of 0.5 mm, a vacuum meniscus set point of 3.5 in. H₂O, and ambient temperature. For LBL deposition, the cartridge and cleaning pad were alternately loaded. Before each deposition, a cleaning cycle consisting of a 3 s purge was applied. Two overprints of each polyelectrolyte were alternately deposited to produce a (PDDA²/PSS²)_z film where z , the total number of repetitions of the 2 × 2 printing program, was varied between 4 and 10.

All samples were aligned and patterns were developed to print lengthwise as to allow for a brief drying moment between printed drops as the printer was repositioned along the y axis. Patterns with lines in both the x and y directions were printed in two separate patterns with sample rotation in between to allow for all lines to be printed in this fashion. All hinged structures were fabricated with lines that are six droplets in width. Although the droplets are delivered at 5 μm intervals, it is estimated that each droplet adds ~50 μm in width to the line. In the case of the multifold structure, (PDDA²/PSS²)₁₀ was printed in one direction before the sample was rotated, and (PDDA²/PSS²)₆ was printed orthogonally. After imaging, four additional layers were deposited so that both hinges had the thickness of (PDDA²/PSS²)₁₀. In the case of the spiral, each hinge was made up of (PDDA²/PSS²)₁₀. The hinges were patterned prior to cutting the spiral structure with a razor blade.

Characterization of Shape Morphing. For humidity-controlled investigation, a quartz chamber 1 in. × 1 in. and 6 in. in height was fabricated to have two openings, one at the very top and one at 3 in. high. Nitrogen was switched on and off at 3 psi where it was allowed to flow into the top opening while the bottom opening remained open to ambient conditions. The chamber was placed on a small square of rubber to minimize leakage. In the case of temperature analysis, a 250 W heat lamp was set up at a distance of 15 cm above the sample. A small magnet was used to hold the sample in place to allow for imaging. Temperature and ambient humidity were monitored with an HI 8064 Hanna Instruments hygrometer. All images were taken with an EOS 20D Cannon digital camera.

■ RESULTS AND DISCUSSION

Stimuli-Responsive LBL Materials. Several features of layer-by-layer (LBL)²⁹-assembled polyelectrolyte multilayers (PEM) make them attractive for solid stimuli-responsive materials that can drive reversible and repeatable shape morphing. First, during the LBL assembly of polyelectrolytes, the formation of polyanion–polycation complexes provides an electrostatically cross-linked structure capable of holding water under ambient conditions.⁴⁷ Changes in environmental humidity drive the sorption and desorption of water, resulting in repeatable and reversible volumetric fluctuations.^{33,47} Second, as a solid material with a Young's modulus, E , around 1 GPa,^{48,49} LBL polyelectrolyte composites provide greater mechanical integrity than, for example, high-performing hydrogels with sub-MPa moduli.⁵⁰ Third, although the increased mechanical integrity of a solid limits the swellability, the nanoscale structural control of LBL assembly may provide the means to allow for optimal volumetric expansion to be realized. When exposed to

the same change in relative humidity, polyelectrolyte films assembled by LBL experienced a greater change in film thickness as compared to complexes prepared by simply mixing the same polyelectrolytes together.^{47,51} Fourth, the presence of nanoscale pores^{52–54} and the success of LBL-based humidity sensors^{55,56} suggest that such dimensional changes may be able to occur rather quickly, as would be desirable for stimuli-responsive structures. Finally, LBL materials are prepared under ambient conditions with nanoscale control over thickness and can be deposited directly into specific patterns without additional processing.⁴⁰ This provides the potential to develop unique patterns easily for the prescribed 2D to 3D transformation of many different materials, including LBL-assembled nanocomposites.

Humidity-Induced Shape Morphing of Nanocomposites. To investigate the performance of LBL polyelectrolyte multilayers as stimuli-responsive materials capable of driving reversible and repeatable shape morphing, poly(diallyldimethylammonium) chloride (PDDA) and poly(sodium 4-styrenesulfonate) were prepared in a bilayer structure with a less-responsive carbon nanotube (CNT) composite. The CNT composite was fabricated by the LBL deposition of 200 layers of cationic polyurethane (PU) and single-walled CNTs. It was removed from its glass substrate, and a thin strip ($15\text{ mm} \times 3\text{ mm}$) was removed to serve as the shape-morphing platform. Inkjet LBL assembly,⁴⁰ an LBL patterning approach that allows for the direct-writing and strictly additive patterning of LBL materials in an accelerated manner, was used to deposit the stimuli-responsive LBL polyelectrolytes selectively onto a CNT strip. In this case, 10 bilayers of $(\text{PDDA}^2/\text{PSS}^2)$ were deposited in a line $\sim 300\text{ }\mu\text{m}$ in width that perpendicularly traversed the entire width of the strip. The PEM was deposited 3 mm into the $15\text{ mm } (\text{PU/CNT})_{200}$ strip, creating a short arm and a long arm separated by a small bilayer that will serve as a hinge to actuate the long arm of the CNT strip (Figure 1). After deposition, there is

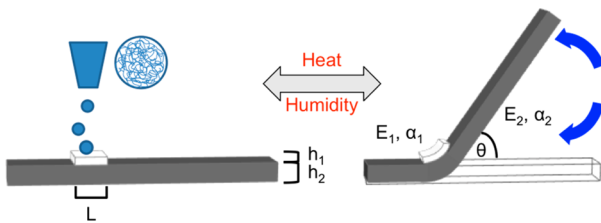


Figure 1. Schematic of the $(\text{PU/CNT})_{200}$ strip with inkjet-deposited $(\text{PDDA}^2/\text{PSS}^2)_{10}$. When exposed to humidity and temperature stimuli, the bimorph responds by bending, creating an angle of deflection of θ in the longer arm. Here, θ depends on the thickness (h), stiffness (E), and expansion coefficient (α) of each layer, along with the total length of the bimorph (L).

no need for additional adhesives or processing because the same electrostatic forces used for their assembly also hold the two layers of the bimorph together. This adhesion will allow for the expansion/contraction of the stimuli-responsive LBL material to apply stress to the CNT layers below, resulting in out-of-plane deformation as the lowest stress configuration is achieved. In fact, before any introduction of controlled stimuli, the stress generated during fabrication as the inkjet deposited $(\text{PDDA}^2/\text{PSS}^2)_{10}$ layers dry on the $(\text{PU/CNT})_{200}$ film is reflected in an initial deflection angle, θ , of $43.9 \pm 1.5^\circ$ at an ambient humidity of 24%. Here, θ is a measurement of the trajectory of the large CNT arm at 0.5 mm with respect to the plane of the short CNT arm.

The stimuli-responsive behavior of the hinged films was first investigated at constant temperature with variations in

environmental humidity. The sample was placed in a quartz chamber, and the shorter arm of the hinged film was weighed down to allow for any out-of-plane actuation of the bilayer hinge to be realized in the long arm of the LBL nanocomposite. The weight was placed no closer than 0.5 mm to the bilayer hinge so as not to influence the location of the fold. A stream of nitrogen was introduced into the chamber to decrease the relative humidity and drive desorption of water from the internal structure of the film. After 5 min (i.e., $t = 5\text{ min}$), the nitrogen exposure led to a greater volumetric contraction of the $(\text{PDDA}/\text{PSS})_{10}$ layer as a result of the desiccation of water. The different extents of contraction in the two layers generates an internal stress that increases the deflection angle of the hinged bilayer to $\theta = 80.9 \pm 1.5^\circ$ (Figure 2A). Upon termination of the nitrogen

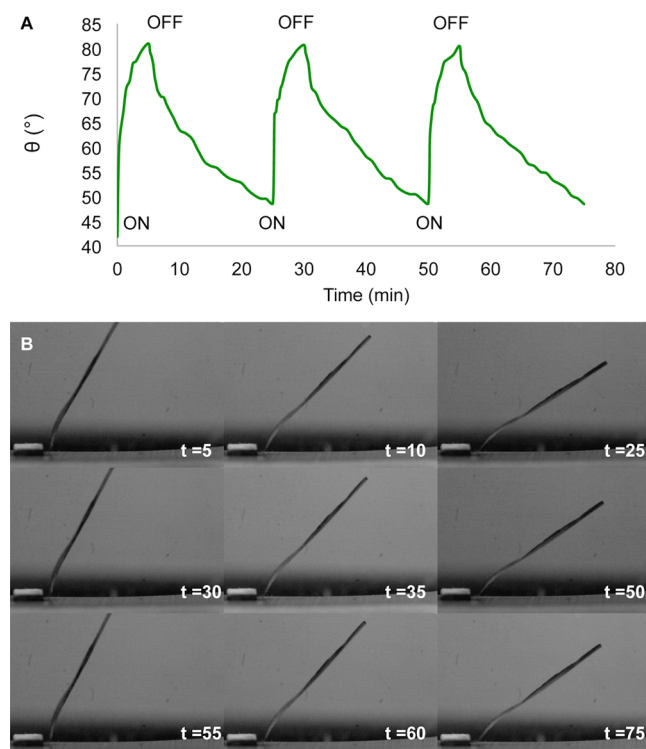


Figure 2. (A) Graphical and (B) image representations of the dependence of the angle of deflection, θ , of the hinged film over time, t . Nitrogen was turned on at $t = 0, 25$, and 50 and turned off at $t = 5, 30$, and 55 . The introduction of nitrogen causes θ to increase, and the removal of nitrogen allows θ to return to a lowered position.

stream, the ambient humid air diffuses into the chamber and hydrates the structure, initiating a decrease in θ . After 20 min ($t = 25\text{ min}$), the nitrogen stream is reintroduced and the cycle is repeated a total of three times for the realization of repeatable and reversible actuation of the bilayer hinge (Figure 2, Movie S1).

Note that whereas the hinged film recovers to $\theta = 49.0 \pm 1.5^\circ$ consistently when exposed to the same conditions, the recovery time of 20 min is not sufficient for a full return to the θ observed immediately after fabrication. However, when allowed to equilibrate for 1 h, the film makes a completely reversible recovery to $\theta = 43$. A range of $9 \pm 1.5^\circ$ as will be employed to investigate temperature-induced shape morphing below.

Temperature-Induced Shape Morphing of Nanocomposites. Next, we investigated the stimuli-responsive behavior of the hinged film in response to temperature, T . As compared to a humidity chamber, the tools used to manipulate temperature

are much more transportable, readily available, and simple, allowing shape-morphing structures that respond to temperature to be highly versatile. Although the response of LBL PEMs has been established for humidity variations,^{31,32,47} their response to temperature variations outside of solution has received little attention. A recent investigation of the thermal response of layered graphene oxide assemblies suggests that materials with nanoscale channels that respond fairly quickly to a decrease in environmental humidity may respond to temperature variations with a pseudonegative thermal expansion (PNTE).⁴³ Here the thermodynamically required decrease in relative humidity with an increase in temperature drives the desiccation of water and a corresponding decrease in dimension that overcomes the intrinsic positive thermal expansion of the material. The fairly quick response to humidity observed in Figure 2A prompted us to investigate (PDPA/PSS) multilayers as a PNTE material for the widespread application of LBL PEMs for temperature-induced shape morphing.

The coefficient of thermal expansion, α , of LBL PEMs was evaluated with a stack of four $(\text{PDPA/PSS})_{250}$ films fabricated with traditional LBL techniques and hot pressed together. The sample was exposed to a temperature ramp of $5\text{ }^\circ\text{C}/\text{min}$ over a ΔT of 30 to $80\text{ }^\circ\text{C}$ while the linear displacement was monitored with a thermal mechanical analyzer (PerkinElmer) (Figure 3A).

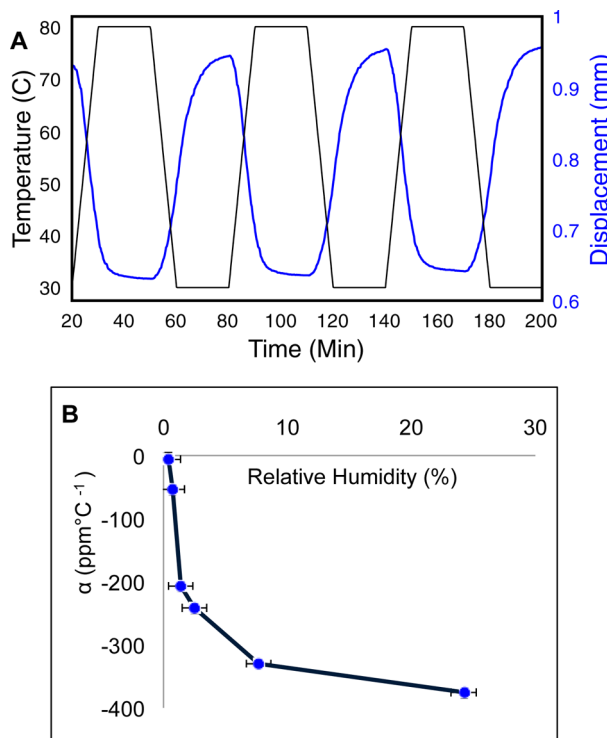


Figure 3. (A) Thermal mechanical analysis of stimuli-responsive LBL PEM showing an apparent negative thermal expansion that reversibly and repeatedly responds. (B) The expansion relies on the relative humidity of the environment. A less-drastic contraction occurs while heating with less available water vapor (relative humidity).

The LBL PEM exhibits a PNTE effect with a repeatable and reversible response to temperature that occurs almost immediately following the environmental change. At an ambient relative humidity of $24 \pm 1\%$, the apparent linear coefficient of thermal expansion of the LBL PEM was calculated to be $\alpha_1 = -368 \pm 9\text{ ppm}/\text{°C}$ over the temperature increase from 35 to $75\text{ }^\circ\text{C}$. The extreme extent of contraction can be realized in comparison

to the LBL CNT composite, which displays an apparent α of only $\alpha_2 = -6.5 \pm 4\text{ ppm}/\text{°C}$ at ambient humidity.

To investigate the role of water, a continuous flux of ultrapure helium was applied during thermal mechanical analysis to decrease the environmental humidity incrementally around the sample. As observed in the graphene oxide assemblies,⁴³ the extent of contraction and apparent α of the LBL polyelectrolyte multilayers became less extreme as the source of water vapor (relative humidity) was decreased (Figure 3B). Also similar to the PNTE graphene oxide assemblies,⁴³ the LBL film shows a quicker dimensional response to heating as compared to cooling. Because unequal water sorption and desorption rates have been predicted in other polyelectrolyte systems,^{57,58} it is likely that water is playing a significant role in this behavior. Even at a relative humidity of 0.37% , the lowest possible humidity that we could obtain within the TMA sample chamber, the LBL PEM still displays a negative expansion coefficient of $-5.3 \pm 2.7\text{ ppm}/\text{°C}$. Although this seems inherently unexpected, previous investigation into the relationship between water content and the expansion of LBL PEMs suggests a complicated mechanism of water sorption where the volumetric expansion is greater than required for the volumetric displacement of the increased water content.⁴⁷ The exaggerated volumetric contraction with increased temperature, along with the quick, reversible, and repeatable response (Figure 3A), makes the LBL PEM an excellent candidate for the active material in a solid, stimuli-responsive bilayer that transforms its shape with temperature stimuli.

To demonstrate the feasibility of temperature-based shape morphing with LBL PEM, the same $(\text{PDPA/PSS})_{10}$ and $(\text{PU/CNT})_{200}$ hinged film actuated above was heated remotely from 20.5 to $37\text{ }^\circ\text{C}$ with a 250 W heat lamp. Because the presence of the CNT composite aids in the efficient absorption of near-IR radiation,²³ the hinged film responds within 5 s of exposure to the lamp, reaching an average peak of $\theta = 79.9 \pm 2^\circ$ within 2 min (Figure 4A). The hinged film recovers completely after 18 min ($t = 20$), when the environmental temperature under the heat lamp returns to $20.5\text{ }^\circ\text{C}$. Subsequent cycles of actuation of the heat lamp show reversible and repeatable shape morphing (Figure 4 and Movie S2). The heat lamp set up provides a faster response than the humidity chamber; however, some instability is realized from the convection currents generated as the surrounding air is heated.

Control of Stimuli-Responsive Architecture. The out-of-plane deformation under ambient humidity is driven by the difference in expansion coefficients ($\alpha_1 = -368 \pm 9\text{ ppm}/\text{°C}$, $\alpha_2 = -6.5 \pm 4\text{ ppm}/\text{°C}$) over the temperature change delivered remotely from the heat lamp of $\Delta T = 16.5\text{ }^\circ\text{C}$. The greater contraction of the $(\text{PDPA/PSS})_{10}$ layer generates a compression stress on the $(\text{PU/CNT})_{200}$ layer of the bimorph hinge, which delivers an opposing tensile stress to the LBL PEM. The material and structural properties of the components allow for the internal stresses within the bilayer hinge to balance through an out-of-plane deformation. Originally derived by Timoshenko,¹⁸ a force balance can be performed to estimate the radius of curvature, ρ , of the bending moment. In the case where the bilayer is employed as a hinge, the unsecured arm can be assumed to follow a trajectory that is tangent to this curvature when in close proximity to the hinge. This tangent extends at an angle of displacement that is geometrically equivalent to the angle subtended by the curved bilayer. Combining Timoshenko's equation for ρ with the geometric definition of arc length allows for the angle of displacement to be expressed in the following manner, where variables m and n are defined as the ratio of layer thickness, h_1/h_2 , and elastic moduli, E_1/E_2 , respectively.

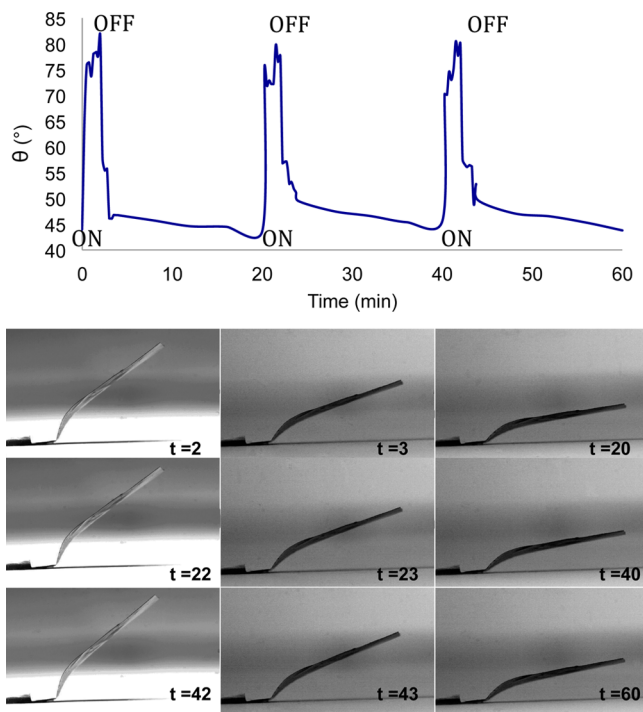


Figure 4. (Top) Graphical and (bottom) image representation of the dependence of the angle of deflection, θ , on temperature variations over time, t . The heat lamp was turned on at $t = 0, 20$, and 40 and turned off at $t = 3, 23$, and 43 .

$$\theta = \frac{L}{\rho} = L \left[\frac{6(\alpha_2 - \alpha_1)(1 + m)^2 \Delta T}{(h_1 + h_2) \left[3(1 + m)^2 + (1 + mn)(m^2 + \frac{1}{mn}) \right]} \right]$$

The theoretical model enables one to investigate and optimize how the angular deflection depends on the material and structural properties of each component. While assuming that n and the value of $(\alpha_2 - \alpha_1)$ remain constant over the temperature range explored, we can mathematically investigate how variations in the thickness of the PEM layer influence θ (Figure 5). From previous studies,^{48,49} E_1 is assumed to be 1 GPa,

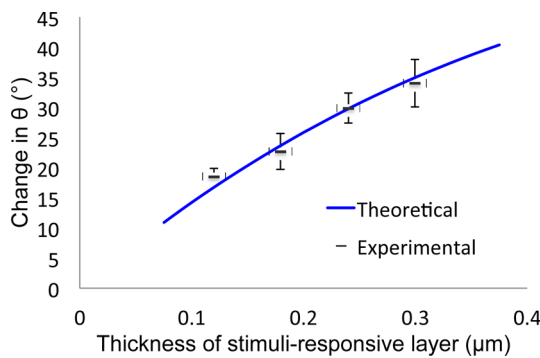


Figure 5. Influence of the thickness, h_1 , of the stimuli-responsive LBL PEM layer on the change in deflection angle, θ , over $\Delta T = 16.5$ °C.

and E_2 and h_2 were measured to be ~ 1.8 GPa and ~ 1.5 μm , respectively. The thickness of the LBL PEM, h_1 , was varied while L was held constant at 300 μm . Here we see that nanoscale control over PEM thickness can provide strict control over the morphology of the actuated structure. One of the many benefits of LBL assembly over alternative composite fabrication

techniques is its nanoscale control over thickness. When the thickness of the PEM layer is varied, the angle of deflection can be strictly controlled as expected by the theoretical analysis (Figure 5). Although the theoretical model assumes that the bilayer is uniformly heated/cooled, curvature is occurring only in one direction and neglects any shear or external forces. Over the range of thicknesses explored, the model fits quite well. For larger temperature ranges, we expect to see larger deflections that eventually will plateau because the PEM layer will be fully dehydrated.

Not only is inkjet LBL capable of controlling the thickness of the stimuli-responsive bilayer, but it can also be used to pattern stresses specifically into localized regions of the nanocomposite. An attractive but relatively unexplored area⁵⁹ is the fabrication of reconfigurable or stimuli-responsive polymeric structures that can fold or unfold in specified patterns. Although theoretical models exist for simple hinge-type structures, the introduction of additional and multidirectional hinges into one structure quickly complicates the balance of internal forces within the nanocomposite. Figure 6A shows a square $(\text{PU/CNT})_{200}$ strip with orthogonal prints of $(\text{PDPA}^2/\text{PSS}^2)_z$ where $z = 10$ is printed in the vertical direction and only $z = 6$ is printed in the horizontal direction. Upon exposure to the heat lamp, the structure folds in a manner where $(\text{PDPA}^2/\text{PSS}^2)_{10}$ dominates and only slight bending is realized across the $(\text{PDPA}^2/\text{PSS}^2)_6$ hinge (Figure 6B). Additional stimuli-responsive material can then be added to make both hinges the same thickness $(\text{PDPA}^2/\text{PSS}^2)_{10}$. As shown on the right, the folded structure of the film is completely different because both hinges provide approximately the same stress on the LBL nanocomposite (Figure 6C). Such structures are of interest because of the numerous applications that can benefit from precise control over 3D actuation. Of possible greater impact, the controllability provided by inkjet LBL opens the door for opportunities to investigate the fundamental mechanics of complex folding so that the development of prescribed 2D to 3D transformations can be widely applied.

In nature, an example of a structure that relies on actuation methods beyond that of a single hinged bimorph is the dispersion mechanisms of awns.¹⁶ Select seeds of grass and wheat have long awns attached to them that aid in dispersing the seeds through a coil and uncoil motion driven by humidity.^{14,15} Here the functionality of the awn is achieved through very subtle yet highly precise twisting movements based on the spatial arrangement of the cellulose fibrils. Although traditional machinery can offer great strengths and frequencies, the ability to make subtle, gentle, and precise movements is often challenging. Materials such as wheat awns serve as a source of inspiration for the design of adaptive and stimuli-responsive materials, with applications in soft robotics.

To investigate the opportunity to create a nanocomposite material capable of a controlled and stimuli-responsive twisting motion, a spiral-like structure was prepared from the LBL nanocomposite, where PEM hinges of $(\text{PDPA}^2/\text{PSS}^2)_{10}$ were specifically patterned onto the corners of the spiral as shown in Figure 7A. When hung within the humidity chamber, the CNT spiral stretches out into a long coil. Upon exposure to nitrogen, the structure responds in a very subtle yet predictable fashion. The stress generated by the bimorph hinges causes the structure to rotate just enough for the central panel to face a different direction before returning back to its original direction when the nitrogen flow is discontinued (Figure 7B and Movie S3). Because LBL serves as a universal approach to the fabrication of nanostructured materials, the simple addition of additional materials to make the structure responsive to multiple stimuli for alternative shape transformations could easily be imagined.

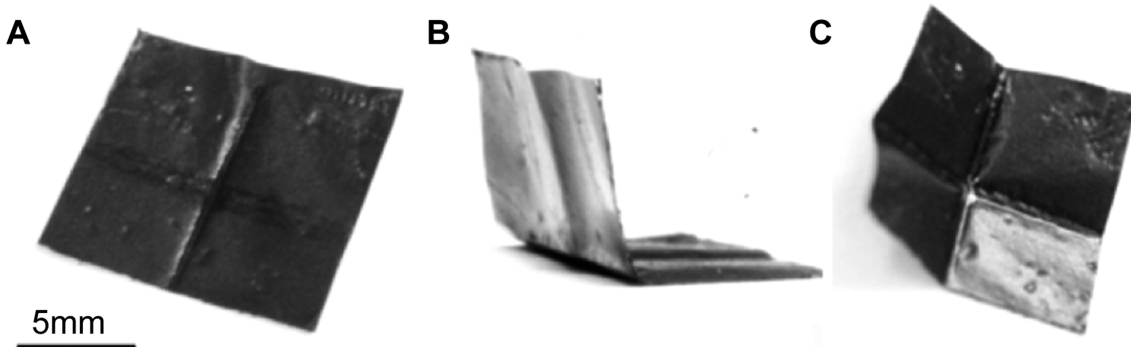


Figure 6. (A) Cross-shaped hinge printed on an LBL nanocomposite square. The vertical hinge is $(\text{PDDA}^2/\text{PSS}^2)_{10}$, and the horizontal hinge is $(\text{PDDA}^2/\text{PSS}^2)_6$. (B) Upon exposure to heat, the structure folds into a structure where the thicker film dominates. (C) The same sample folds into a shape with equal curvature at the hinge with the addition of extra layers of PEM to make both vertical and horizontal hinges the same thickness. This demonstrates control of the final shape based on the number of layers deposited at the hinge.

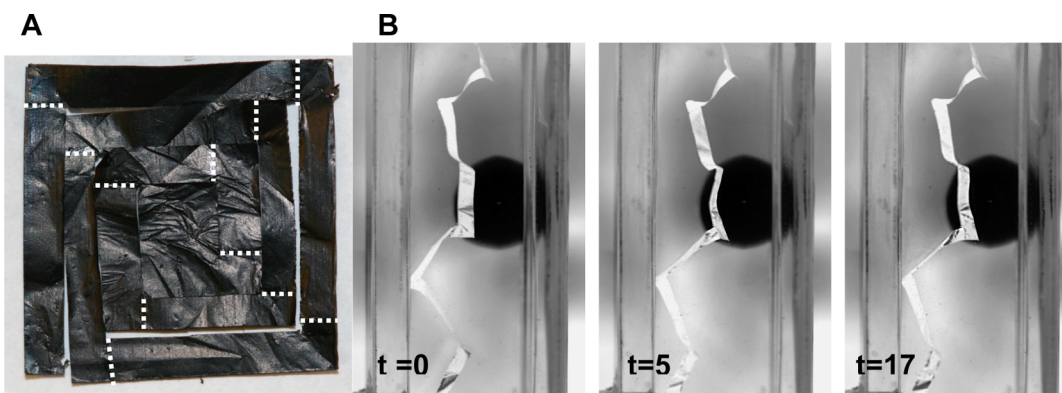


Figure 7. (A) A spiral is cut into an LBL nanocomposite that has stimuli-responsive hinges inkjet printed into the edges of the spiral (drawn in as dotted lines). The complete structure is 1 in² when flat. (B) When hung from a support and introduced to nitrogen, the structure responds with reversible and subtle twisting motion. Nitrogen is turned on at $t = 0$ and off at $t = 17$ s.

CONCLUSIONS

Nature frequently produces solid materials capable of repeatedly and reversibly transforming shape in response to variations in environmental temperature and humidity. Mimicking these motions achieved in nature in synthetic materials provides opportunities for inducing controllable motion into LBL nanocomposites. LBL PEMs provide stimuli-responsive swelling with changes in humidity that also allow for actuation based on temperature due to the PNTE.⁴³ When patterned with inkjet technology on a CNT nanocomposite, the two form a bimorph structure capable of controllable and reversible shape transformations with fairly advanced complexity.

A number of challenges remain for both the theoretical and experimental front of shape-morphing structures. Furthermore, integration with diverse materials is required to enable electronic, optical, and biomedical functionalities. Widespread application will require further miniaturization and scaling of the self-folding mechanisms. In terms of theoretical challenges, further investigation into the mechanism of swelling, especially in the case of PNTE, will need to be developed for the optimization of responsive behavior. The application of LBL and inkjet technology, however, serves as a promising approach to addressing several of these challenges based on the high level of structural control granted with the combination of the two technologies.

ASSOCIATED CONTENT

S Supporting Information

Actuation of the bilayer hinge. Shape morphing. This material is available free of charge via the Internet at <http://pubs.acs.org>.

AUTHOR INFORMATION

Corresponding Author

*E-mail: kotov@umich.edu.

Notes

The authors declare no competing financial interest.

Biographies



Christine M. Andres received her Ph.D. in chemical engineering from the University of Michigan in Ann Arbor in 2013 under the direction of Prof. Kotov. During her graduate studies, she was awarded the National Science Foundation Graduate Fellowship and the Intel PhD Corporate Fellowship. Her research interests are additive manufacturing and advanced materials. She is currently a senior research engineer at 3M.



Jian Zhu received his B.S. in chemical engineering from Tianjin University and Nankai University in China. He obtained his Ph.D. in chemical engineering from the University of Michigan in Ann Arbor in 2013 under the direction of Prof. Kotov. His research interests are hierarchical composites with electronics and energy applications. He is currently a postdoctoral fellow at Northwestern University.



Terry Shyu received B.S. degrees in (1) materials science and engineering and (2) engineering and public policy from Carnegie Mellon University. Her research interests are composite materials with reconfigurable functionalities. She is currently pursuing her Ph.D. in materials science and engineering at the University of Michigan in Ann Arbor.



Connor Flynn received his B.S. in chemical engineering from the University of Michigan in Ann Arbor in 2013. During his senior year, he worked as an undergraduate research assistant in the Kotov laboratory. His research interests are in functional nanocomposites. He is now working at First Solar, Inc.



Nicholas A. Kotov is the Joseph B. and Florence V. Cejka Professor of Chemical Engineering at the University of Michigan in Ann Arbor, holding joint appointment in biomedical engineering, materials science and engineering, chemical engineering, and macromolecular science and engineering. He received his M.S. (1987) and Ph.D. (1990) under the guidance of M. Kuzmin of the chemistry department at Moscow State University. He worked as a postdoctoral associate at Syracuse University in the group of J. Fendler. Prior to his current position, he was a professor at Oklahoma State University. His group at the University of Michigan is actively involved in research in the field of nanostructured materials, nanomaterial assembly, and functional composites for biomedical and energy applications.

■ ACKNOWLEDGMENTS

This study was partially supported by the Center for Solar and Thermal Energy Conversion, an Energy Frontier Research Center funded by the U.S. Department of Energy, Office of Science, Office of Basic Energy Sciences under award number DE-SC0000957. We acknowledge support from the NSF via grants ECS-0601345, EFRI-BSBA 0938019, CBET 0933384, CBET 0932823, and CBET 1036672. The work is also partially supported by AFOSR MURI 444286-P061716 and NIH 1R21CA121841-01A2. This research was supported by NSF DMR-9871177 and DMR-0315633 grants. We acknowledge EMAL facilities at the University of Michigan.

■ REFERENCES

- (1) Stuart, M. A. C. Emerging applications of stimuli-responsive polymer materials. *Nat. Mater.* **2010**, *9*, 101–113.
- (2) Shenoy, V. B.; Gracias, D. H. Self-folding thin-film materials: from nanopolyhedra to graphene origami. *MRS Bull.* **2012**, *37* (), 847–854.
- (3) Leong, T. G.; Zarafshar, A. M.; Gracias, D. H. Three-dimensional fabrication at small size scales. *Small* **2010**, *6* (), 792–806.
- (4) Leng, J. Shape-memory polymers and their composites: stimulus methods and applications. *Prog. Mater. Sci.* **2011**, *56* (), 1077–1135.
- (5) Gibson, P. Humidity-dependent air permeability of textile materials. *Text. Res. J.* **1999**, *69*, 311–317.
- (6) Menges, A.; Reichert, S. Material capacity: embedded responsiveness. *Architectural Design* **2012**, *52*–59.
- (7) Fernandes, R.; Gracias, D. H. Self-folding polymeric containers for encapsulation and delivery of drugs. *Adv. Drug Delivery Rev.* **2012**, *64* (), 1579–1589.
- (8) Ilievski, F. Soft robotics for chemists. *Angew. Chem., Int. Ed.* **2011**, *50*, 1890–1895.

- (9) Vaia, R.; Baur, J. Adaptive composites. *Science* **2008**, *319*, 420–421.
- (10) Erb, R. M.; Sander, J. S.; Grisch, R.; Studart, A. R. Self-shaping composites with programmable bioinspired microstructures. *Nat. Commun.* **2013**, *4*, 1712.
- (11) Ionov, L. Biomimetic 3D self-assembling biomicroconstructs by spontaneous deformation of thin polymer films. *J. Mater. Chem.* **2012**, *22*, 19366–19375.
- (12) Dawson, J.; Vincent, J. F. V.; Rocca, A. M. How pine cones open. *Nature* **1997**, *390*, 668–668.
- (13) Harrington, M. J.; Razghandi, K.; Ditsch, F.; Guidicci, L.; Rueggeberg, M.; Dunlop, J. W. C.; Fratzl, P.; Neinhuis, C.; Burgert, I. Origami-like unfolding of hydro-actuated ice plant seed capsules. *Nat. Commun.* **2011**, *2*.
- (14) Stamp, N. E. Efficacy of explosive vs hygroscopic seed dispersal by an annual grassland species. *Am. J. Bot.* **1989**, *76* (), 555–561.
- (15) Peart, M. H. Experiments on the biological significance of the morphology of seed-dispersal units in grasses. *J. Ecol.* **1979**, *67*, 843–863.
- (16) Elbaum, R. The role of wheat awns in the seed dispersal unit. *Science* **2007**, *316*, 884–886.
- (17) Reyssat, E.; Mahadevan, L. Hygromorphs: from pine cones to biomimetic bilayers. *J. R. Soc., Interface* **2009**, *6*, 951–957.
- (18) Timoshenko, S. Analysis of bi-metal thermostats. *J. Opt. Soc. Am. Rev. Sci. Instrum.* **1925**, *11*, 233–255.
- (19) Shim, T. S. Controlled origami folding of hydrogel bilayers with sustained reversibility for robust microcarriers. *Angew. Chem., Int. Ed.* **2012**, *51*, 1420–1423.
- (20) Luchnikov, V.; Sydorenko, O.; Stamm, M. Self-rolled polymer and composite polymer/metal micro- and nanotubes with patterned inner walls. *Adv. Mater.* **2005**, *17*, 1177.
- (21) Schild, H. G. Poly(n-isopropylacrylamide) - experiment, theory and application. *Prog. Polym. Sci.* **1992**, *17* (), 163–249.
- (22) Jager, E. W. H.; Inganäs, O.; Lundstrom, I. Microrobots for micrometer-size objects in aqueous media: potential tools for single-cell manipulation. *Science* **2000**, *288*, 2335–2338.
- (23) Zhang, X. B. Optically- and thermally-responsive programmable materials based on carbon nanotube-hydrogel polymer composites. *Nano Lett.* **2011**, *11*, 3239–3244.
- (24) Tokarev, I.; Minko, S. Stimuli-responsive hydrogel thin films. *Soft Matter* **2009**, *5*, 511–524.
- (25) Hu, Z. B.; Zhang, X. M.; Li, Y. Synthesis and application of modulated polymer gels. *Science* **1995**, *269*, 525–527.
- (26) Stoychev, G. Hierarchical multi-step folding of polymer bilayers. *Adv. Funct. Mater.* **2013**, *23*, 2295–2300.
- (27) Ma, M. M. Bio-inspired polymer composite actuator and generator driven by water gradients. *Science* **2013**, *339*, 186–189.
- (28) Urban, M. W. *Handbook of Stimuli-Responsive Materials*; Wiley-VCH: Weinheim, Germany, 2011.
- (29) Decher, G. Fuzzy nanoassemblies: toward layered polymeric multicomposites. *Science* **1997**, *277*, 1232–1237.
- (30) Sukhishvili, S. A. Responsive polymer films and capsules via layer-by-layer assembly. *Curr. Opin. Colloid Interface Sci.* **2005**, *10*, 37–44.
- (31) Shen, L. Y. Humidity responsive asymmetric free-standing multilayered film. *Langmuir* **2010**, *26*, 16634–16637.
- (32) Ma, Y.; Sun, J. Q. Humido- and thermo-responsive free-standing films mimicking the petals of the morning glory flower. *Chem. Mater.* **2009**, *21*, 898–902.
- (33) Ma, Y.; Zhang, Y.; Wu, B.; Sun, W.; Li, Z.; Sun, J. Polyelectrolyte multilayer films for building energetic walking devices. *Angew. Chem., Int. Ed.* **2011**, *50*, 6254–6257.
- (34) Tang, Z.; Wang, Y.; Podsiadlo, P.; Kotov, N. A. Biomedical applications of layer-by-layer assembly: from biomimetics to tissue engineering. *Adv. Mater.* **2006**, *18*, 3203–3224.
- (35) Tang, Z. Nanostructured artificial nacre. *Nat. Mater.* **2003**, *2* (), 413–U8.
- (36) Podsiadlo, P.; Kaushik, A. K.; Arruda, E. M.; Waas, A. M.; Shim, B. S.; Xu, J.; Nandivada, H.; Pumplin, B. G.; Lahan, J.; Ramamoorthy, A.; Kotov, N. A. Ultrastrong and stiff layered polymer nanocomposites. *Science* **2007**, *318*, 80–83.
- (37) Mamedov, A. A.; Kotov, N. A.; Prato, M.; Guldi, D. M.; Wicksted, J. P.; Hirsch, A. Molecular design of strong single-wall carbon nanotube/polyelectrolyte multilayer composites. *Nat. Mater.* **2002**, *1*, 190–194.
- (38) Hammond, P. T. Form and function in multilayer assembly: new applications at the nanoscale. *Adv. Mater.* **2004**, *16*, 1271–1293.
- (39) Kotov, N. A. Layer-by-Layer Assembly of Nanoparticles and Nanocolloids: Intermolecular Interactions, Structure and Materials Perspectives. In *Multilayer Thin Films*; Wiley-VCH: Weinheim, Germany, 2003; pp 207–243.
- (40) Andres, C. M.; Kotov, N. A. Inkjet deposition of layer-by-layer assembled films. *J. Am. Chem. Soc.* **2010**, *132*, 14496–14502.
- (41) Andres, C. M.; Fox, M. L.; Kotov, N. A. Traversing material scales: macroscale LBL-assembled nanocomposites with microscale inverted colloidal crystal architecture. *Chem. Mater.* **2012**, *24*, 9–11.
- (42) Andres, C. M.; Larraza, I.; Corrales, T.; Kotov, N. A. Nanocomposite microcontainers. *Adv. Mater.* **2012**, *24*, 4597–4600.
- (43) Zhu, J.; Andres, C. M.; Xu, J.; Ramamoorthy, A.; Tsotsis, T.; Kotov, N. A. Pseudonegative thermal expansion and the state of water in graphene oxide layered assemblies. *ACS Nano* **2012**, *6*, 8357–8365.
- (44) Nishino, T. All-cellulose composite. *Macromolecules* **2004**, *37*, 7683–7687.
- (45) Nogi, M. Optically transparent nanofiber paper. *Adv. Mater.* **2009**, *21*, 1595–1598.
- (46) Jain, A.; Vijayan, K. Kevlar 49 fibres: thermal expansion coefficients from high temperature X-ray data. *Curr. Sci.* **2000**, *78*, 331–335.
- (47) Kohler, R.; Donch, I.; Ott, P.; Laschewsky, A.; Fery, A.; Krastev, R. Neutron reflectometry study of swelling of polyelectrolyte multilayers in water vapors: influence of charge density of the polycation. *Langmuir* **2009**, *25*, 11576–11585.
- (48) Hsieh, M. C.; Farris, R. J.; McCarthy, T. J. Mechanical properties of layer-by-layer-deposited polyelectrolyte assemblies. *Abstr. Pap. Am. Chem. Soc.* **1999**, *218*, U620–U620.
- (49) Gao, C.; Donath, E.; Dudnik, V.; Möhwald, H. Elasticity of hollow polyelectrolyte capsules prepared by the layer-by-layer technique. *Eur. Phys. J. E* **2001**, *5*, 21–27.
- (50) Tanaka, Y.; Gong, J. P.; Osada, Y. Novel hydrogels with excellent mechanical performance. *Prog. Polym. Sci.* **2005**, *30*, 1–9.
- (51) De, S.; Cramer, C.; Schonhoff, M. Humidity dependence of the ionic conductivity of polyelectrolyte complexes. *Macromolecules* **2011**, *44*, 8936–8943.
- (52) Jin, W. Q.; Toutianoush, A.; Tieke, B. Size- and charge-selective transport of aromatic compounds across polyelectrolyte multilayer membranes. *Appl. Surf. Sci.* **2005**, *246*, 444–450.
- (53) Liu, X. Y.; Bruening, M. L. Size-selective transport of uncharged solutes through multilayer polyelectrolyte membranes. *Chem. Mater.* **2004**, *16*, 351–357.
- (54) Chavez, F. V.; Schonhoff, M. Pore size distributions in polyelectrolyte multilayers determined by nuclear magnetic resonance cryoporometry. *J. Chem. Phys.* **2007**, *126*, 7.
- (55) Yu, H.-h.; Yao, L.; Wang, L.-x.; Hu, W.-b.; Jiang, D.-s. Fiber optic humidity sensor based on self-assembled polyelectrolyte multilayers. *J. Wuhan Univ. Technol., Mater. Sci. Ed.* **2001**, *16*, 65–69.
- (56) Su, P. G.; Cheng, K. H. Self-assembly of polyelectrolytic multilayer thin films of polyelectrolytes on quartz crystal microbalance for detecting low humidity. *Sens. Actuators, B* **2009**, *142*, 123–129.
- (57) Ge, S. Absorption, desorption, and transport of water in polymer electrolyte membranes for fuel cells. *J. Electrochem. Soc.* **2005**, *152*, A1149.
- (58) Tosto, S. Water adsorption/desorption in proton-conducting ionomer membranes: the model case of sulfonated and silylated poly-ether-ether-ketone. *Solid State Ionics* **2012**, *209–210*, 9–14.
- (59) Kim, J.; Hanna, J. A.; Byun, M.; Santangelo, C. D.; Hayward, R. C. Designing responsive buckled surfaces by halftone gel lithography. *Science* **2012**, *335*, 1201–1205.